

# Power Spectrum Computation for an Arbitrary Phase Noise Using Middleton's Convolution Series: Implementation Guideline and Experimental Illustration

Pierre Brochard, Thomas Südmeyer, *Member, IEEE*, and Stéphane Schilt

**Abstract**—In this paper, we revisit the convolution series initially introduced by Middleton several decades ago to determine the power spectrum (or spectral line shape) of a periodic signal from its phase noise power spectral density. This topic is of wide interest, as it has an important impact on many scientific areas that involve lasers and oscillators. We introduce a simple guideline that enables a fairly straightforward computation of the power spectrum corresponding to an arbitrary phase noise. We show the benefit of this approach on a computational point of view, and apply it to various types of experimental signals with different phase noise levels, showing a very good agreement with the experimental spectra. This approach also provides a qualitative and intuitive understanding of the power spectrum corresponding to different regimes of phase noise.

**Index Terms**—Convolution, laser noise, phase noise, spectral analysis.

## I. INTRODUCTION

MANY scientific areas rely today on stable and low-noise optical or microwave oscillators. For instance, ultranarrow-linewidth cavity-stabilized lasers are a key element in optical atomic clocks that have surpassed the best microwave frequency standards in terms of fractional frequency stability in the last decade [1], [2]. Such lasers have also produced microwave signals with the lowest phase noise to date by optical-to-microwave frequency division using an optical frequency comb [3], [4]. Other types of frequency-stabilized lasers with less stringent frequency stability requirements are used in microwave atomic clocks [5] or in optical sensing applications, e.g., in differential absorption lidars for the monitoring of pollutants or greenhouse gases in the atmosphere [6]. Low-noise microwave signals are needed, for example, in radar systems, large baseline interferometry, or in telecommunications and time synchronization. When dealing with low-noise oscillators, it is primordial to characterize their noise properties. This is also the case for other types of lasers with a higher noise (broader linewidth), even for free-running laser sources in some cases.

This work was supported by the European Union's Seventh Framework Programme for research, technological development and demonstration through the Marie-Curie International Training Network Project Future Atomic Clock Technologies under Grant PITN GA 2013 607493. (Corresponding author: Pierre Brochard.)

The authors are with the Laboratoire Temps-Fréquence, Université de Neuchâtel, CH-2000 Neuchâtel, Switzerland (e-mail: pierre.brochard@unine.ch; thomas.sudmeyer@unine.ch; stephane.schilt@unine.ch).

Digital Object Identifier 10.1109/TUFFC.2017.2747620

The most complete quantity to characterize the noise of an oscillator is the phase noise power spectral density (PN-PSD)  $S_\phi(f)$  or the frequency noise power spectral density (FN-PSD)  $S_\nu(f)$ , which are directly related to each other by the well-known relation  $S_\nu(f) = f^2 S_\phi(f)$ , where  $f$  is the offset frequency (or Fourier frequency). However, other simpler values are often preferred by the scientific community to characterize and compare oscillators such as the integrated phase noise  $\phi_{\text{rms}}$  or the full width at half maximum of the oscillator power spectrum. Therefore, it is important to understand how these values can be obtained from an experimental noise spectrum.

A simple method to retrieve the linewidth of an oscillator (e.g., a laser) directly from its FN-PSD without first calculating the corresponding power spectrum was proposed by Domenico *et al.* [7]. The method is easy to implement and proved to be accurate to better than 10% in a large range of laser linewidths spanning from kilohertz to megahertz that were experimentally studied [8]. Moreover, this method provides a simple estimation of the feedback bandwidth that is required in a stabilization loop, such as a phase-locked loop (PLL), to suppress the linewidth of the oscillator and achieve a tight lock characterized by the presence of a coherent peak in the spectrum. However, this approach does not provide any information about the shape of the spectrum. Furthermore, its experimental verification was performed in a regime of high phase noise that leads to a finite spectral linewidth, but the method has not yet been evaluated in a low phase noise regime (with  $\phi_{\text{rms}}$  in the range of 1 rad), where larger discrepancies are expected.

The problem of determining the power spectrum of a carrier subjected to an arbitrary phase noise has been a topic of interest for a long time. In the 1950's, Middleton [9], [10] first reported theoretical considerations about the power spectrum corresponding to a signal modulated by stationary random disturbances, especially in the case of a Gaussian noise. In this frame, he introduced a series of convolution products of the PN-PSD that is referred to as Middleton's expansion series. Following this initial work, various theoretical studies have been reported based on Middleton's expansion series applied to other types of noise spectra [11]–[13]. All these works primarily concerned the case of modulated electrical oscillators, for instance, for radio, TV, and other kinds of communications signals. They generally dealt either with the

limiting case of Middleton’s expansion obtained for small-integrated phase noise values, or with the different case of large-integrated phase noise described by Woodward’s theorem [14], [15], respectively.

Thirty years after Middleton’s initial work, Elliott *et al.* [16] discussed, for the first time, the general mathematical expression to determine the power spectrum of an optical oscillator, i.e., a laser, from its PN-PSD. As an outcome, the exact linewidth of the laser can be extracted. Elliott’s theoretical description is basically similar to Middleton’s prior work, but it has been much more spread and used in the laser community, whereas Middleton’s work remains poorly known today in this area. The main difference between the two approaches, which will be reviewed in Section II, lies in the fact that Elliott’s formula requires the autocorrelation function of the oscillator phase to be calculated, as well as its exponential form, whereas Middleton used an expansion series of this term. Elliott’s approach appeared more natural after the universalization of the fast Fourier transform algorithm [17] that was unknown at the time of Middleton’s initial work, and which is necessary to compute Elliott’s formula. Implementing this formula requires a two-step integration that needs to be performed numerically. A notable exception is the ideal case of an infinite white frequency noise PSD that can be analytically solved, leading to a Lorentzian line shape described by the Schawlow–Townes–Henry linewidth [18], [19]. In the general case, the numerical integration is not easy to implement and some care is required to retrieve the correct line shape without introducing numerical artifacts [8]. Therefore, the process is not straightforward and can be fairly time-consuming, not in terms of pure computational time, but to determine the proper computation parameters as will be discussed in Section III-B. Furthermore, this approach does not provide an intuitive understanding of the shape of the power spectrum retrieved for a given PN-PSD.

At first glance, Middleton’s expansion series may appear inappropriate for practical implementation due to its infinite number of terms. So far, it has been applied essentially in the extreme situation of low phase noise ( $\phi_{\text{rms}} \ll 1$ ), whereas the opposite situation of high phase noise ( $\phi_{\text{rms}} \gg 1$ ) has been independently described by Woodward’s theorem [14], [15] and the central limit theorem [20]. In both situations, the power spectrum can be determined or approximated. However, the applicability of Middleton’s series in the more general case of an intermediate phase noise regime has not been reported so far to the best of our knowledge. A reason is that there was no recognized universal criterion enabling an easy determination of the number of terms of the series that need to be calculated to obtain the proper power spectrum [11]–[13].

In this paper, we revisit Middleton’s expansion and implement it to calculate the power spectra corresponding to different types of PN-PSD. As an important outcome, we theoretically show that only a limited number of terms of the expansion series have a significant contribution to the power spectrum, and these relevant terms only depend on the integrated phase noise, but not on the shape of the PN-PSD. As a result, we give a simple guideline to apply Middleton’s

series to an arbitrary noise, which is valid for any integrated phase noise and type of PN-PSD. We also discuss the benefits of Middleton’s series over the usual integration of Elliott’s formula to calculate and understand the power spectrum of an oscillator subjected to an arbitrary noise. Middleton’s series provides an intuitive comprehension of some characteristic spectral features that appear in the power spectrum for a given PN-PSD. It predicts not only the presence of a coherent peak at the carrier frequency, surrounded by some sideband noise components occurring in the well-known regime of low integrated phase noise, but it also gives insights to understand and qualitatively describe the evolution of the spectrum from a coherent peak to a broader bell-shaped spectrum that occurs when the integrated phase noise increases. This bell-shaped profile tends to a Gaussian spectrum when the variance of the PN-PSD is finite according to the central limit theorem. Such an intuitive understanding cannot be directly obtained from Elliott’s general formula.

This paper is organized as follows. In Section II, we will start by a short review of the basic theoretical concepts that link the PN-PSD to the power spectrum, introducing Elliott’s general formula and then deriving the less known Middleton’s expansion. In Section III, we will explain how to implement Middleton’s expansion in practice, based on a simple criterion that we introduce to determine the number of terms of the series that need to be considered in the computation. As an example of application, we will highlight some advantages provided by Middleton’s expansion, which circumvents numerical artifacts that can occur with the use of Elliott’s formula. Then, we will show how Middleton’s expansion series enables understanding the shape of the power spectrum. Finally, we will present, in Section IV, some experimental results obtained from real signals that illustrate the different theoretical aspects considered in the previous sections and demonstrate the appropriateness of Middleton’s approach to compute power spectra from the PN-PSD of different signals.

## II. THEORETICAL BACKGROUND

We remind in this section the main theoretical aspects leading to the formulas previously derived by Middleton [10] and Elliott *et al.* [16], respectively, which link the power spectrum of a signal to its PN-PSD. The two formulas derive from the exact same formalism, which is known for a long time and commonly used in the community [7], [21], [22]. We do not introduce new theoretical aspect, the novelty of our work being presented in the following sections. However, we estimated important to first review the main steps of the derivation of Elliott’s and Middleton’s formulas. The only difference between these two expressions occurs in their final form, as Middleton’s expansion appears as a Taylor series of Elliott’s general formula.

An ideal (noise-free) oscillator at frequency  $\nu_0$  is characterized in the spectral domain by a Dirac function. However, a real oscillator is affected by some phase noise and is mathematically described by the following expression:

$$E(t) = E_0 \sin[2\pi \nu_0 t + \phi(t)] \quad (1)$$

where  $E_0$  is the amplitude of the signal (the electrical field in the case of a laser),  $\nu_0$  is the carrier frequency, and  $\phi(t)$  describes the temporal phase fluctuations. The power spectrum  $S_E(\nu - \nu_0)$  of this signal corresponds to the Fourier transform (written as  $\mathcal{F}[\cdot]$ ) of the autocorrelation function  $R_E(\tau) = \langle E(t) \cdot E(t + \tau) \rangle$  of the signal (where  $\langle \cdot \rangle$  denotes an ensemble average)

$$S_E(\nu - \nu_0) = \mathcal{F}[R_E(\tau)]. \quad (2)$$

In the case where the phase variations  $[\phi(t + \tau) - \phi(\tau)]$  constitute a stationary random process with Gaussian distribution and zero mean value as generally encountered [22], the autocorrelation function  $R_E(\tau)$  of the signal can be obtained from the autocorrelation function of the phase  $R_\phi(\tau) = \langle \phi(t) \cdot \phi(t + \tau) \rangle$  through the following expression [16], [21], [22]:

$$R_E(\tau) = E_0^2 \cdot e^{R_\phi(\tau) - R_\phi(0)} = E_0^2 \cdot e^{R_\phi(\tau)} \cdot e^{-R_\phi(0)}. \quad (3)$$

The autocorrelation function of the phase evaluated at a time delay  $\tau$  corresponds to the Fourier transform of the PN-PSD  $S_\phi(f)$

$$R_\phi(\tau) = \int_0^{+\infty} S_\phi(f) \cdot \cos(2\pi f \tau) df \quad (4)$$

whereas its value for  $\tau = 0$  corresponds to the squared integrated phase noise  $\phi_{\text{rms}}^2$

$$R_\phi(0) = \int_0^{+\infty} S_\phi(f) df = \phi_{\text{rms}}^2. \quad (5)$$

Equations (4) and (5) mathematically involve an integration from zero to infinity, which may diverge on either side, e.g., at zero in the case of  $1/f^2$  or  $1/f^3$  PN-PSD. However, we are interested in this work in physical experimental signals, which are always observed over a finite time interval, so that these integrals remain finite. By combining (2) to (5) and taking into account the properties of Fourier transforms ( $\mathcal{F}[\alpha] = \alpha\delta(x)$  where  $\alpha$  is a constant and  $\delta(x)$  is the Dirac function, and  $\mathcal{F}[x \cdot y] = \mathcal{F}[x] * \mathcal{F}[y]$ , where  $*$  denotes the convolution product), the following expression is obtained for the power spectrum:

$$\begin{aligned} S_E(\nu - \nu_0) &= E_0^2 e^{-\phi_{\text{rms}}^2} \delta(\nu) * \mathcal{F}[e^{R_\phi(\tau)}] \\ &= E_0^2 e^{-\phi_{\text{rms}}^2} \delta(\nu) * \mathcal{F}[e^{\int_0^{+\infty} S_\phi(f) \cdot \cos(2\pi f \tau) df}]. \end{aligned} \quad (6)$$

We refer to this expression as Elliott's formula, as it was first introduced by Elliott *et al.* [16] to describe the spectrum of a laser. It links the power spectrum  $S_E(\nu - \nu_0)$  to the PN-PSD  $S_\phi(f)$  via a two-step integration process, described by (2) and (4). This integration can be solved only numerically in most cases, which makes the shape of the power spectrum not intuitive for a given PN-PSD. Some critical points for the implementation of this numerical integration must be considered, as will be discussed in Section III-B. Elliott's formula can be transformed into a more convenient form by exploiting the series expansion of the exponential function

$$e^{R_\phi(\tau)} = \sum_{n=0}^{\infty} \frac{R_\phi^n(\tau)}{n!} = 1 + R_\phi(\tau) + \sum_{n=2}^{\infty} \frac{R_\phi^n(\tau)}{n!}. \quad (7)$$

This mathematical development is valid for any phase noise. As a physical experimental signal has a finite integrated phase noise  $\phi_{\text{rms}}$  as previously mentioned, the infinite series (7) converges in practice. By introducing the series expansion (7) into Elliott's general formula (6), and taking into account the properties of Fourier transforms ( $\mathcal{F}[x + y] = \mathcal{F}[x] + \mathcal{F}[y]$  and  $\mathcal{F}[x \cdot y] = \mathcal{F}[x] * \mathcal{F}[y]$ ), the following expression is obtained for the power spectrum, which is valid for any real noise type and magnitude:

$$\begin{aligned} S_E(\nu - \nu_0) &= E_0^2 e^{-\phi_{\text{rms}}^2} \delta(\nu) \\ &+ E_0^2 e^{-\phi_{\text{rms}}^2} S_\phi(f) \\ &+ E_0^2 e^{-\phi_{\text{rms}}^2} \sum_{n=2}^{\infty} \frac{1}{n!} S_\phi(f) *^{n-1} S_\phi(f). \end{aligned} \quad (8)$$

This expression is characterized by an infinite series of self-convolution products of the PN-PSD of different orders  $n$ , denoted by the symbol  $*^n$ . We refer to this expression as Middleton's expansion, as it was first introduced by Middleton [10]. In contrast to Elliott's general formula that first requires the phase autocorrelation function (4) to be computed for a large number of values of the time delay  $\tau$ , Middleton's approach directly deals with multiple self-convolution products of the double-sideband PN-PSD  $S_\phi(f)$ , which are easier to compute and do not depend on the particular choice of some computational parameters. The price to pay is that the expansion series contains an infinite number of terms, which has prevented its implementation in other cases than the extreme condition of small integrated phase noise. We will show in the following section that only a limited number of terms have a significant contribution to the spectrum for finite values of  $\phi_{\text{rms}}$  (which is always the case experimentally as previously explained) and we will provide a simple guideline for the numerical implementation of Middleton's expansion for an arbitrary PN-PSD.

The decomposition in different convolution products occurring in Middleton's expansion will also enable us to qualitatively describe the shape of the power spectrum, which is not so easy with Elliott's general formula. By analyzing Middleton's expression (8), one notices that the fundamental term of the series (order  $n = 0$ ) is a delta (Dirac) function centered at the carrier frequency  $\nu_0$ . The amplitude of this term ( $E_0^2 e^{-\phi_{\text{rms}}^2}$ ) depends on the squared integrated phase noise. This delta function corresponds to the commonly called coherent peak. This term is always present in the series, but its amplitude is significant only when the signal has a low integrated phase noise, typically in the range of 1 rad or smaller, otherwise its exponential decay with respect to  $\phi_{\text{rms}}^2$  makes it negligible [22]. The important parameter to assess the presence of a coherent peak is its relative power, i.e., the ratio between the carrier power and the integrated signal power, which corresponds to  $e^{-\phi_{\text{rms}}^2}$ . For instance, for an integrated phase noise  $\phi_{\text{rms}} = 2$  rad, approximately 2% of the signal power is contained in the coherent peak. It is experimentally possible to observe it using a spectrum analyzer with a sufficiently high resolution.

The first-order term ( $n = 1$ ) of Middleton's expansion (8) is directly proportional to the PN-PSD and is located on each side



TABLE I  
FIRST TERMS OF MIDDLETON'S EXPANSION IN A SERIES  
OF PN-PSD SELF-CONVOLUTION PRODUCTS

Order $n = 0$	$E_0^2 e^{-\phi_{\text{rms}}^2} \delta(v)$
Order $n = 1$	$E_0^2 e^{-\phi_{\text{rms}}^2} S_\phi(f)$
Order $n = 2$	$\frac{1}{2} E_0^2 e^{-\phi_{\text{rms}}^2} S_\phi(f) * S_\phi(f)$
Order $n = 3$	$\frac{1}{6} E_0^2 e^{-\phi_{\text{rms}}^2} S_\phi(f) * S_\phi(f) * S_\phi(f)$

of the coherent peak centered at  $\nu_0$ . This term is the dominant contribution, besides the zeroth order term responsible for the coherent peak, in the low phase noise regime ( $\phi_{\text{rms}} \ll 1$ ) as well-known from textbooks on the subject [22]. The higher order terms ( $n > 1$ ) correspond to higher order convolution products. Their expression for the terms of lowest orders ( $n = 0, 1, 2, 3$ ) is listed in Table I.

### III. COMPUTATION OF MIDDLETON'S EXPANSION

#### A. Practical Implementation of Middleton's Expansion

Middleton's expansion (8) is made of an infinite series of convolution products of the PN-PSD. The number of terms to be considered to accurately compute the power spectrum depends on their respective weight, which is characterized by the relative power contained in each term, i.e., its integrated value or area  $A_n$  (moment of order 0)

$$A_0 = e^{-\phi_{\text{rms}}^2}$$

$$A_n = e^{-\phi_{\text{rms}}^2} \frac{1}{n!} \int S_\phi(f) *^{n-1} S_\phi(f) df, \quad \text{for } n > 0. \quad (9)$$

To calculate the relative power of each term of the series, one makes use of the following general property of the convolution products: the integral  $A[y(x)]$  of any function  $y(x)$  corresponding to the convolution product of two functions  $g(x)$  and  $f(x)$ ,  $y(x) = g(x) * f(x)$ , is equal to the product of the areas of the two functions:  $A[y(x)] = A[g(x)] \cdot A[f(x)]$ . Applying this property to the self-convolution product of order  $n > 0$  of a function  $h(x)$ ,  $y(x) = h(x) *^{n-1} h(x)$ , leads to  $A[y(x)] = (A[h(x)])^n$ . In our case, the considered function is the phase noise spectrum  $S_\phi(f)$  and its area corresponds to the squared integrated phase noise  $A[S_\phi(f)] = \phi_{\text{rms}}^2$ . Therefore,  $A[S_\phi(f) *^{n-1} S_\phi(f)] = A[S_\phi(f)]^n = (\phi_{\text{rms}}^2)^n$  and the relative power contained in the term of order  $n$  of Middleton's series (8) is given by

$$A_n = e^{-\phi_{\text{rms}}^2} \frac{(\phi_{\text{rms}}^2)^n}{n!}. \quad (10)$$

This expression indicates that the relative power of each term of order  $n$  of Middleton's series follows a Poisson distribution that is independent of the amplitude and shape of the phase noise spectrum  $S_\phi(f)$ , but depends only on the squared integrated phase noise  $\phi_{\text{rms}}^2$ . Summing the relative power  $A_n$  of all terms with  $n > 0$  leads to a value of  $(1 - e^{-\phi_{\text{rms}}^2})$  that corresponds to the total power of the signal out of the coherent peak.

The Poisson distribution has a median value that is very close to  $\phi_{\text{rms}}^2$  and a variance rigorously equal to  $\phi_{\text{rms}}^2$ , so that its

width (standard deviation) corresponds to  $\phi_{\text{rms}}$ . This distribution tends to a normal (Gaussian) distribution centered at  $\phi_{\text{rms}}^2$  with a variance  $\phi_{\text{rms}}^2$  at high integrated phase noise. In this case, one can determine the term of maximum order  $n_{\text{max}}$  that needs to be taken into account in Middleton's series to accurately determine the power spectrum, by requiring that the cumulated contribution (in terms of relative power) of all higher order terms that are neglected is smaller than a given tolerance factor  $\varepsilon$ . Using the cumulative distribution function of the Gaussian distribution, the following expression is obtained:

$$n_{\text{max}} = \lfloor \phi_{\text{rms}}^2 + \phi_{\text{rms}} \sqrt{-2 \cdot \ln(\varepsilon)} \rfloor \quad (11)$$

where the symbol  $\lfloor \cdot \rfloor$  represents the nearest integer, but  $n_{\text{max}} \geq 1$  in all cases. The first-order term  $n = 1$  is always considered in addition to the coherent peak given by  $n = 0$  when the argument in the nearest integer function in (11) is smaller than 0.5. The simple parameter  $n_{\text{max}}$  can be straightforwardly and unambiguously determined prior to the spectrum computation for any PN-PSD. Equation (11) is strictly valid for a Gaussian distribution, i.e., in the case of high integrated phase noise values. However, it remains a very good approximation also for a Poisson distribution, i.e., in the general case of any integrated phase noise values as shown in the following.

With this criterion, Middleton's series of convolution products is fairly easy to implement for any noise spectrum. Such a simple condition has not been proposed before to the best of our knowledge. From our numerous experimental observations (see some examples in Section IV) and considering the cumulative distribution function of the Poisson distribution, a tolerance factor  $\varepsilon = 1\%$  is sufficient to accurately compute the power spectrum from the PN-PSD, as more than 98.4% of the total signal power is contained in the considered terms for any value of  $\phi_{\text{rms}}$ . This fraction increases even up to  $\sim 99.86\%$  for a Gaussian distribution of the relative power of the different terms of Middleton's series that is obtained at high  $\phi_{\text{rms}}$ . With  $\varepsilon = 1\%$ , the previous expression (11) can be transformed into the simpler following formula that involves only the integrated phase noise:

$$n_{\text{max}} = \lfloor \phi_{\text{rms}}^2 + 3\phi_{\text{rms}} \rfloor. \quad (12)$$

A double-sideband PN-PSD must be used in the computation of Middleton's expansion to retrieve a correct power spectrum. The PN-PSD must be known with the same spectral resolution as targeted for the power spectrum. Furthermore, we used the following recurrence relation to calculate the successive convolution orders:

$$S_\phi(f) *^n S_\phi(f) = S_\phi(f) * [S_\phi(f) *^{n-1} S_\phi(f)]. \quad (13)$$

#### B. Benefit of Middleton's Approach Over Elliott's Formula

To compare the use of Middleton's expansion with Elliott's general formula for the computation of power spectra, we first considered a rectangular PN-PSD bounded between 700 Hz and 1 kHz and of amplitude  $S_\phi^0 = 0.01 \text{ rad}^2/\text{Hz}$  as displayed in Fig. 1(a) (corresponding to  $\phi_{\text{rms}}^2 = 3 \text{ rad}^2$ ). Very similar results

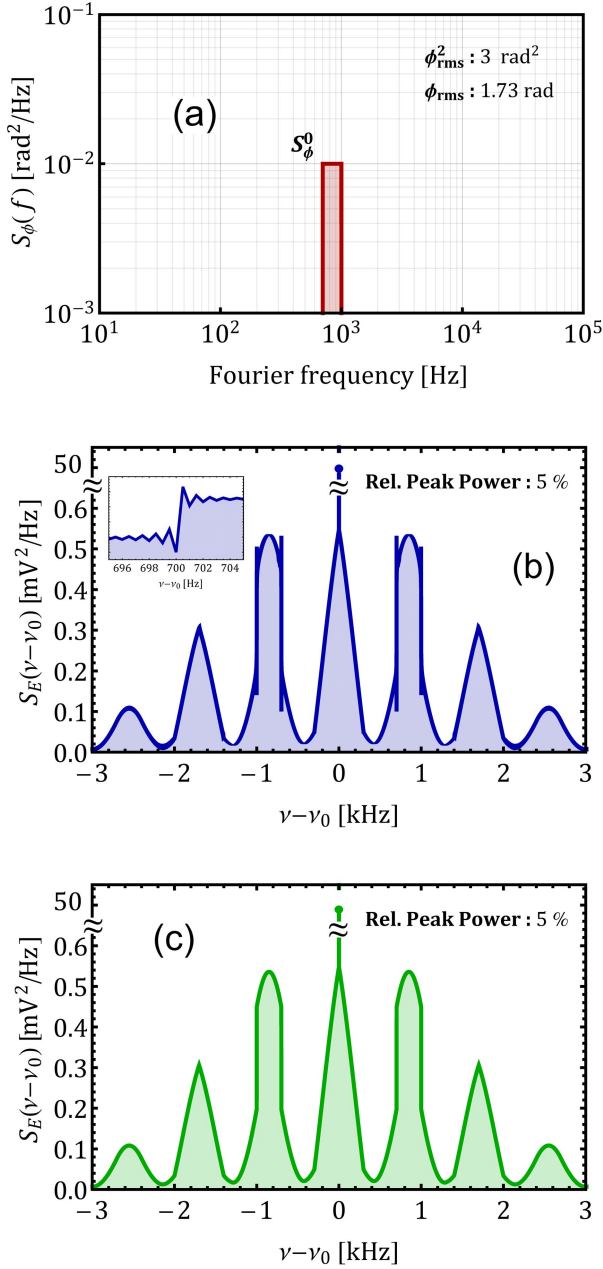


Fig. 1. Comparison of the power spectra computed using Elliott's general formula (by Fourier transform of the autocorrelation function) and Middleton's expansion method (using a series of convolution products). (a) PN-PSD used in the simulations, made of a rectangular narrowband noise centered at 850 Hz with a bandwidth of 300 Hz and an amplitude of  $0.01 \text{ rad}^2/\text{Hz}$  (integrated phase noise of 1.73 rad). (b) Power spectrum retrieved with Elliott's standard method. (Inset) Zoomed-in-view on Gibbs' artifact [23]–[26] occurring at the rectangular transition of the first sideband resulting from the Fourier transform involved in Elliott's standard method. (c) Power spectrum retrieved using Middleton's convolution products expansion.

are numerically obtained for the same resolution bandwidth of 1 Hz using Elliott's formula [see Fig. 1(b)] and Middleton's expansion series [see Fig. 1(c)] computed up to the term of order  $n_{\max} = 8$  according to our reported criterion (12). In both cases, the coherent peak reaches  $\approx 50 \text{ mV}^2/\text{Hz}$  (here  $E_0 = 1 \text{ V}$ ) and similar sidebands (same shape, same amplitude) are observed at the various harmonics of the noise center frequency  $f_0$ . However, the spectrum obtained using Elliott's formula, which involves a Fourier transform, presents

some oscillations at the transition of the rectangular part of the first-order sidebands [see inset of Fig. 1(b)]. These oscillations constitute a computational artifact, which is a typical effect of Fourier transforms known as Gibbs' phenomenon [23]–[26]. The spectrum obtained using Middleton's expansion is not affected by such artifact and is more accurate. The numerical implementation of Elliott's formula to simulate the power spectrum corresponding to an arbitrary PN-PSD is not a straightforward procedure. Great care is required in this implementation to retrieve a correct spectral line shape. The method requires the autocorrelation function of the signal to be calculated from the PN-PSD for an ensemble of correlation times  $\tau$ . Therefore, the integral (4) needs to be computed a large number of times for different values of  $\tau$ . The overall range of values of the correlation time  $\tau$  and the sampling rate of the autocorrelation function must be properly set to obtain the correct spectrum line shape by Fourier transform (2), but they cannot be chosen fully independently. An improper choice of these parameters may lead to numerical artifacts, resulting in an incorrect spectrum. We illustrate this effect with a real example shown in Fig. 2. For this purpose, we generated an experimental test signal using a waveform generator frequency-modulated by a bandpass-filtered white noise (more details about the experimental conditions will be given in Section IV). We measured both the PN-PSD of this signal [Fig. 2(a)] and its power spectrum using a phase noise analyzer (FSWP26 from Rohde & Schwarz). We also separately computed the corresponding power spectrum using both Elliott's formula and Middleton's expansion series [see Fig. 2(c)]. The computation of Elliott's formula requires the autocorrelation function of the phase of the signal to be calculated in a first step according to (4). The result is shown in Fig. 2(b). When only the central part of this signal in the range of  $\pm 0.1 \text{ s}$  was considered in the Fourier transform (2), a correct power spectrum was retrieved, similar to the measured spectrum (not show in the figure). However, the resulting spectral resolution was only 10 Hz in this case. To achieve a 1-Hz resolution that is straightforwardly obtained using Middleton's expansion, the autocorrelation function needs to be considered in a larger range of  $\pm 1 \text{ s}$ . In this case, an erroneous power spectrum was obtained as illustrated in Fig. 2(c), which results from artifacts occurring in the autocorrelation function at  $|\tau| > 0.2 \text{ s}$ . In contrast, Middleton's series computed up to the term of order  $n_{\max} = 10$  (for an integrated phase noise  $\phi_{\text{rms}} = 2 \text{ rad}$ ) is in excellent agreement with the experimental spectrum measured with a 1-Hz resolution.

For the computation of Elliott's formula, the choice of the  $\tau$  values is not trivial as the spectrum to be retrieved is not known *a priori*, and may require an iterative process. Therefore, this process may be fairly time-consuming. On the opposite, the number of terms of Middleton's expansion series to be used in the computation is unambiguously determined prior to the calculation according to our simple expression (12). Then, the computation only requires multiple self-convolution products of the PN-PSD, which may be simpler and faster to implement, and circumvents some artifacts that can occur in the computation of Elliott's formula.

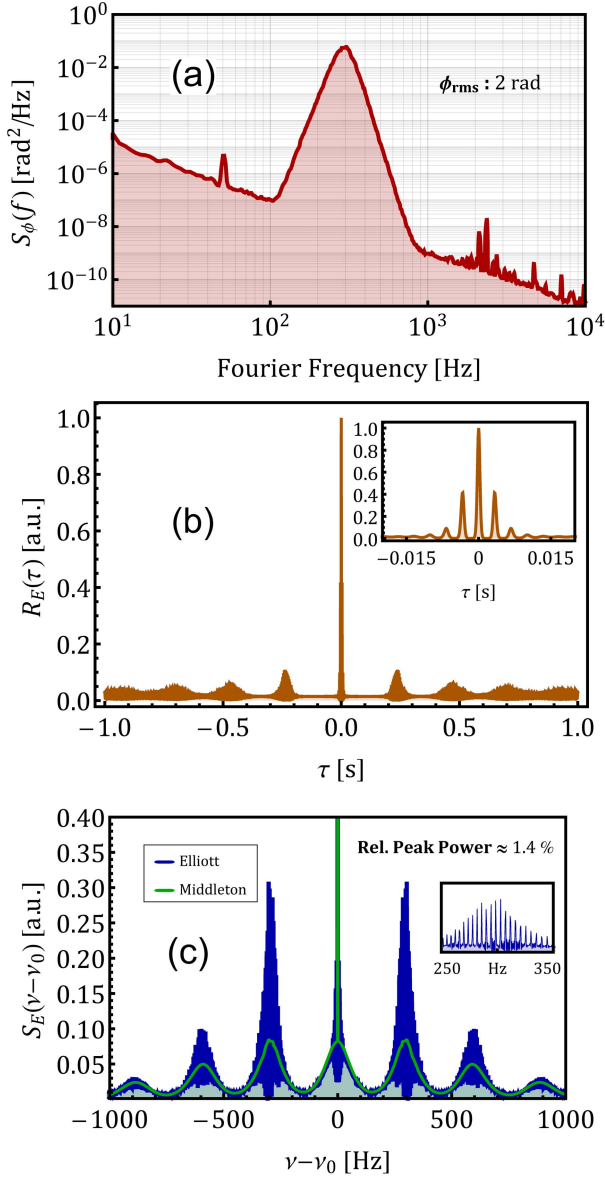


Fig. 2. Example of artifact that can occur in the computation of the power spectrum using Elliott's formula, in comparison with the use of Middleton's expansion series. (a) Experimental PN-PSD used in the computations, which was delivered by a waveform generator frequency-modulated by a bandpass-filtered white noise (with an integrated phase noise of 2 rad). (b) Autocorrelation function calculated from (4) and used in Elliott's formula. (Inset) Zoomed-in-view on the central part ( $-0.02$  to  $0.02$  s). (c) Power spectrum retrieved using Middleton's expansion (green line) and Elliott's formula (blue line). The measured experimental spectrum, not displayed here for the clarity of the plot, coincides with the spectrum obtained with Middleton's series. (Inset) Zoomed-in-view on the graph between 250 and 350 Hz showing the discrepancies obtained with the computation of Elliott's formula.

### C. Qualitative Power Spectrum Description

Computing the power spectrum with Middleton's expansion has the major advantage that the shape of the spectrum can be qualitatively explained. It also elucidates the transformation of the power spectrum from a zero-linewidth coherent peak to a broader bell-shaped spectrum at increasing integrated phase noise.

By looking at the individual terms of Middleton's series of convolution products (8), the resulting shape of the power

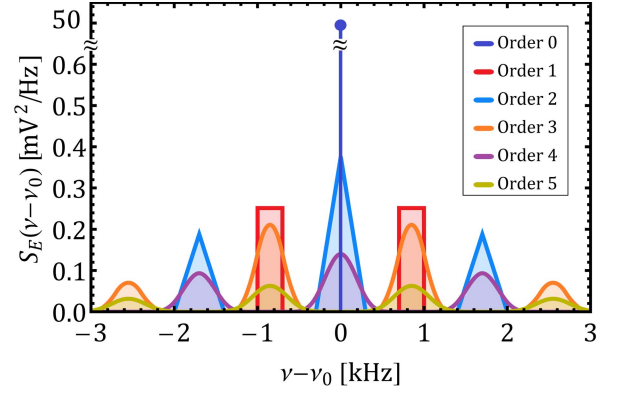


Fig. 3. First six individual terms of Middleton's series computed for a rectangular PN-PSD as displayed in Fig. 1(a). Dark blue, blue, and violet lines are even-order terms ( $n = 0, 2, 4$ ). Red, orange, and yellow lines are odd-order terms ( $n = 1, 3, 5$ ).

spectrum can be clearly understood as illustrated in Fig. 3. Here, the same rectangular PN-PSD as shown in Fig. 1(a) was considered, with a relatively low integrated phase noise of 1.73 rad. The first six terms of lowest orders ( $n = 0$  to 5) of Middleton's series are displayed on the plot; their mathematical form follows the expressions listed in Table I. The coherent peak in the center of the spectrum (dark blue line) corresponds to the zeroth-order term. The first-order term ( $n = 1$ ) is directly proportional to the PN-PSD, it has the same rectangular shape centered at  $\pm f_0$  (dark red line). The second order term ( $n = 2$ ) corresponds to the convolution of the PN-PSD with itself, resulting into a triangular shape (blue line). The PN-PSD being double-sideband, three triangular functions are obtained: one is located at the carrier frequency and two sidebands of halved amplitude are located at  $\pm 2f_0$ . The third-order component ( $n = 3$ ) is made of Gaussian-like (bell-shaped) sidebands centered at  $\pm f_0$  and  $\pm 3f_0$  (orange line) that results from the convolution between a rectangle and a triangle. Similarly, higher order terms tend more and more toward Gaussian sidebands centered at various harmonics of the noise frequency  $f_0$ . The complete power spectrum is the sum of all individual components, leading to a spectrum similar to Fig. 1(c), made of sidebands of different shapes (e.g., a triangle at  $\nu = \nu_0$  and  $\nu = \nu_0 \pm 2f_0$ , two deformed rectangles at  $\nu_0 \pm f_0$ ). An important remark here is that even-order terms of the convolution series have a maximum value at the center of the spectrum, but odd-order terms do not. For an integrated phase noise of 10 rad, the Poisson distribution (10) of the relative power contained in each mode of Middleton's series shows that the low order convolution products become totally negligible and the terms of order  $n \approx 100$  are dominant. A high order self-convolution of any signal with a PN-PSD bounded between  $f_{\min} > 0$  and  $f_{\max} < \infty$ , such that its variance (moment of order 2) is finite, tends toward a Gaussian distribution according to the central limit theorem [20]. Furthermore, the sum of several weighted Gaussian curves remains Gaussian-like. Therefore, it becomes clear that any PN-PSD produces a Gaussian-like (or bell-shaped) spectrum as illustrated in Fig. 4 as soon as its integrated phase noise is relatively



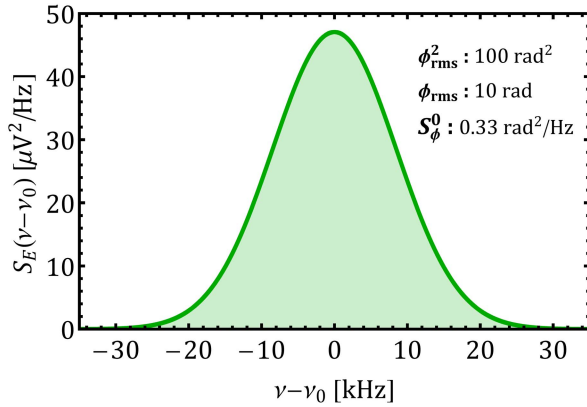


Fig. 4. Power spectrum computed using Middleton’s series (8) with  $n_{\max} = 130$  terms according to (12) for a rectangular PN-PSD with a high integrated phase noise of 10 rad, leading to a Gaussian distribution.

large, typically higher than some radians in the aforementioned example of a rectangular PN-PSD. However, the transition to a Gaussian-like spectrum may occur at higher  $\phi_{\text{rms}}$  values for other types of PN-PSD. This result was already known from Woodward’s theorem, which states that the spectrum of a high-index frequency-modulated waveform is approximated by the probability distribution of the modulating wave shifted by the carrier frequency [14], [15]. This leads to a Gaussian spectrum in the case of a high integrated phase noise, independently of the use of Middleton’s series. However, this approximation is valid only in the case of a high-integrated noise. The advantage of the use of Middleton’s series that we revisit in this paper is its applicability to any integrated phase noise condition.

In complement to our previous theoretical considerations (see Section III-A and earlier in the present section), we numerically confirmed the validity of the transition to a Gaussian-like spectrum at high integrated phase noise for a large number of PN-PSD of various shapes and amplitudes, such as bounded flicker phase noise, white phase noise, or more “exotic” noise PSDs. An example is shown in Fig. 5(a) for an arbitrarily distributed PN-PSD with two different amplitudes corresponding to an integrated phase noise of 2 and 6 rad, respectively. In the first case [Fig. 5(b)], a coherent peak is apparent in the power spectrum, surrounded by some bumps at  $\approx \pm 3$  kHz which are induced by the noise bump also present in the PN-PSD. This case mimics a real situation encountered in a stabilization loop, for instance a PLL to stabilize an oscillator onto a reference signal, which produces such a servo bump both in the PN-PSD and in the power spectrum. In the second case with a higher integrated phase noise of 6 rad [Fig. 5(c)], the computed power spectrum has a Gaussian shape as explained before, as the dominant orders of the convolution products series are fairly large (around 36 here), so that the high-order self-convolution terms of the PN-PSD tend toward a Gaussian distribution. This example shows that the regime of high integrated phase noise leading to a Gaussian power spectrum occurs already for  $\phi_{\text{rms}}$  values of a few radians in this case (typically  $\phi_{\text{rms}} > \pi$ ).

#### IV. EXPERIMENTAL ILLUSTRATIONS AND TESTS

In Sections II and III, we have shown how to compute the power spectrum of a signal from its PN-PSD based on

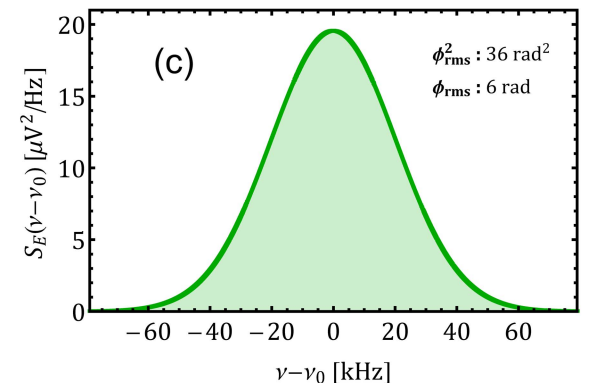
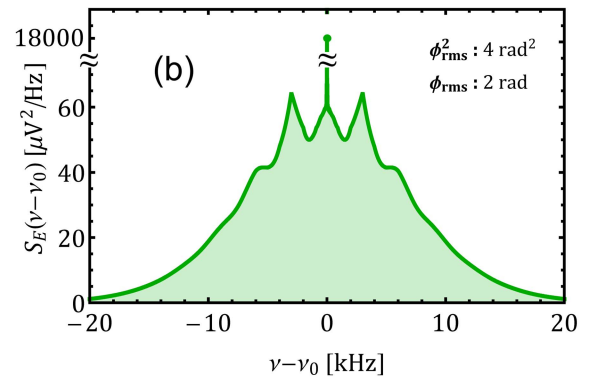
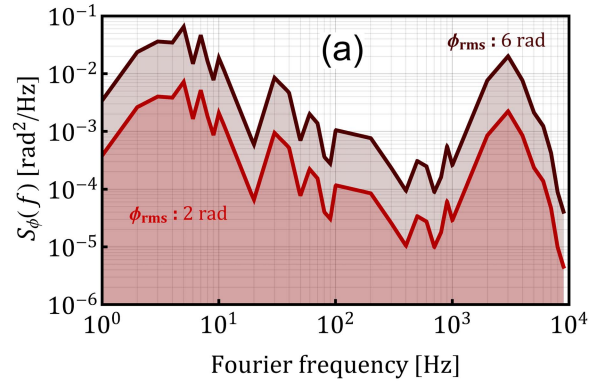


Fig. 5. Power spectrum determination using Middleton’s expansion series for an arbitrarily distributed PN-PSD with two different amplitudes ( $\phi_{\text{rms}} = 2$  rad and  $\phi_{\text{rms}} = 6$  rad, respectively). (a) Arbitrary PN-PSD considered in the simulations. (b) and (c) Corresponding power spectra computed using Middleton’s series (8) up to the order  $n_{\max} = 10$  and  $n_{\max} = 54$ , respectively, according to (12).

Middleton’s series of convolution products. Here, we present experimental results that illustrate the different aspects previously addressed on the theoretical point of view for the implementation of Middleton’s series. In particular, these results confirm the suitability of the relationship (12) that we have introduced to determine the number of terms of the infinite series to be taken into account in the computation. In a first illustrative example, we will present the dependence of the relative power of the coherent peak as a function of the integrated phase noise that was discussed in Section II, in the cases of low and intermediate integrated phase noises. Then, we will apply Middleton’s series to different types of

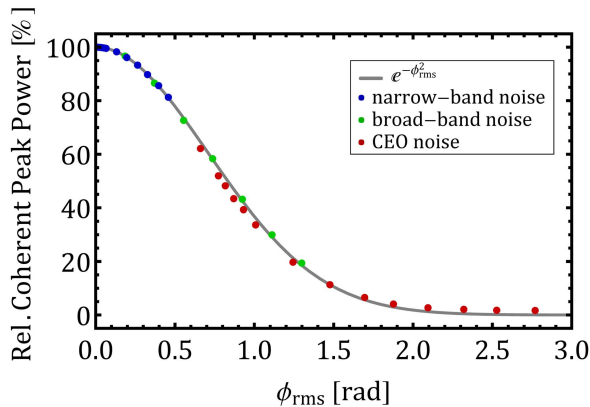


Fig. 6. Experimental validation of the dependence of the relative power contained in the coherent peak as a function of the integrated phase noise. Results were obtained for three different types of noise: from signals generated by a frequency-modulated synthesizer with different bandwidths of the induced noise (blue and green dots) and from the CEO beat of an optical frequency comb (red dots). The gray curve represents the theoretical dependence  $e^{-\phi_{rms}^2}$ .

experimental PN-PSD covering the regimes of low, intermediate, and high integrated phase noise. In all cases, we will show the excellent agreement obtained in comparison with experimentally measured power spectra.

#### A. Relative Power of the Coherent Peak

A function generator (Agilent 33250A) modulated in frequency by an external voltage was used to generate various types of PN-PSD with a different integrated phase noise. The external voltage was tailored by filtering a white noise source by a narrowband filter made of two cascaded tunable high-pass and low-pass filters (Stanford Research Systems SIM965) to generate PN-PSDs that approximate the ideal rectangular noise considered in the previous simulations [see Fig. 1(a)]. The cut-off frequencies of the high-pass and low-pass filters were first adjusted at  $\sim 600$  and  $\sim 800$  Hz, respectively, to produce a narrowband noise. Then, the cut-off frequencies were shifted to 3 (high-pass) and 8 kHz (low-pass) to generate a broader PN-PSD. In both cases, the noise level was varied to achieve different values of  $\phi_{rms}$ . In addition, we also used the “real” signal of the carrier envelope offset (CEO) beat of a commercial self-referenced optical frequency comb (FC1500 from Menlo Systems, Germany). More details about the use of this system are given in Section IV-B. In all cases, both the PN-PSD and the power spectrum of the signals under test were measured using a phase noise analyzer (FSWP26 from Rohde & Schwarz). Fig. 6 shows the dependence of the relative power of the coherent peak as a function of the integrated phase noise. An excellent agreement is observed between the experimental points obtained for the different aforementioned signals at various noise levels and the theoretical curve  $e^{-\phi_{rms}^2}$  obtained from the first term of Middleton’s expansion series (order 0 in Table I).

#### B. Test of Middleton’s Power Spectra Computation

We have experimentally tested the computation of Middleton’s series (8) restricted to the number of terms defined by our

formula (12) and compared the results with actual spectra. For this purpose, we used the CEO beat signal of our frequency comb as a test signal. As this signal was relatively noisy and did not allow us to directly achieve the phase noise regimes of interest for this paper, we frequency-divided it by a factor 16 or 4 using frequency prescalers (RF Bay FPS-16-4 or FPS-4-20, respectively). Changing the servo-controller gain in the CEO stabilization loop enabled different shapes of PN-PSD and various values of integrated phase noise to be obtained. To achieve the regime of low phase noise, we directly used the output signal at  $\sim 10$  MHz of a frequency synthesizer (HP 3314A). These three different cases corresponding to low, intermediate, and high phase noise values are displayed in Fig. 7. Based on our previous theoretical considerations discussed in Section III, we can define a more precise delimitation between these different noise regimes compared to the two extreme cases that are generally considered (i.e., low noise for  $\phi_{rms} \ll 1$  and high noise for  $\phi_{rms} \gg 1$ ). In the case of low phase noise characterized by a power spectrum consisting of a coherent peak surrounded on each side by the PN-PSD  $S_\phi(f)$  [22], only the terms  $n = 0$  and 1 of Middleton’s expansion series (8) contribute to the spectrum. Therefore, we chose to consider  $\phi_{rms}^2 + 3\phi_{rms} < 1.5$  in (12) as an upper limit for this regime, which roughly corresponds to  $\phi_{rms} < \pi/8$ . In this low phase noise regime, one has  $n_{max} = 1$ , meaning that only the two terms  $n = 0$  and  $n = 1$  are considered in Middleton’s series. In this case, at least 85% of the signal power is contained in the coherent peak and more than 98.9% in the two first components  $n = 0$  and  $n = 1$  [calculated from (10)]. For integrated phase noise values larger than  $\sim \pi/8$  rad, more terms of Middleton’s series need to be taken into account ( $n_{max} \geq 2$ ) to determine the correct power spectrum. We have shown at the end of Section III-C that the regime of high phase noise leading to a bell-shaped envelope spectrum occurs already at a phase noise of a few radians, due to the smoothing behavior of the convolution product. We define the lower limit of this noise regime as  $\phi_{rms} > \pi$ . In this case, less than 0.06% of the signal power is contained in the coherent peak, and at least 20 terms of Middleton’s series need to be considered to accurately compute the power spectrum, which corresponds to a minimum accuracy of 99.5% in terms of the total power of the retrieved spectrum. The range of intermediate phase noise corresponds to  $\pi/8 < \phi_{rms} < \pi$ , i.e., to  $20 > n_{max} \geq 2$  in terms of the maximum order term in Middleton’s series. It leads to a more complex shape of the power spectrum, which is obtained with a relative power accuracy comprised between 98.88% and 99.94%.

For each of our experimental signals, we measured both the PN-PSD and the power spectrum using the same phase noise analyzer as in the previous section. From the measured PN-PSD, we also computed the corresponding power spectrum using Middleton’s expansion (8) up to a term of maximum order  $n_{max}$  given by (12). In the considered examples,  $n_{max} = 1, 7,$  and  $31,$  respectively, for integrated phase noise values  $\phi_{rms} \approx 0.4, 1.45,$  and  $4.22$  rad. We compared the result of the simulations (green lines in Fig. 7) with the directly measured power spectra (blue lines), obtaining an excellent agreement in all cases.



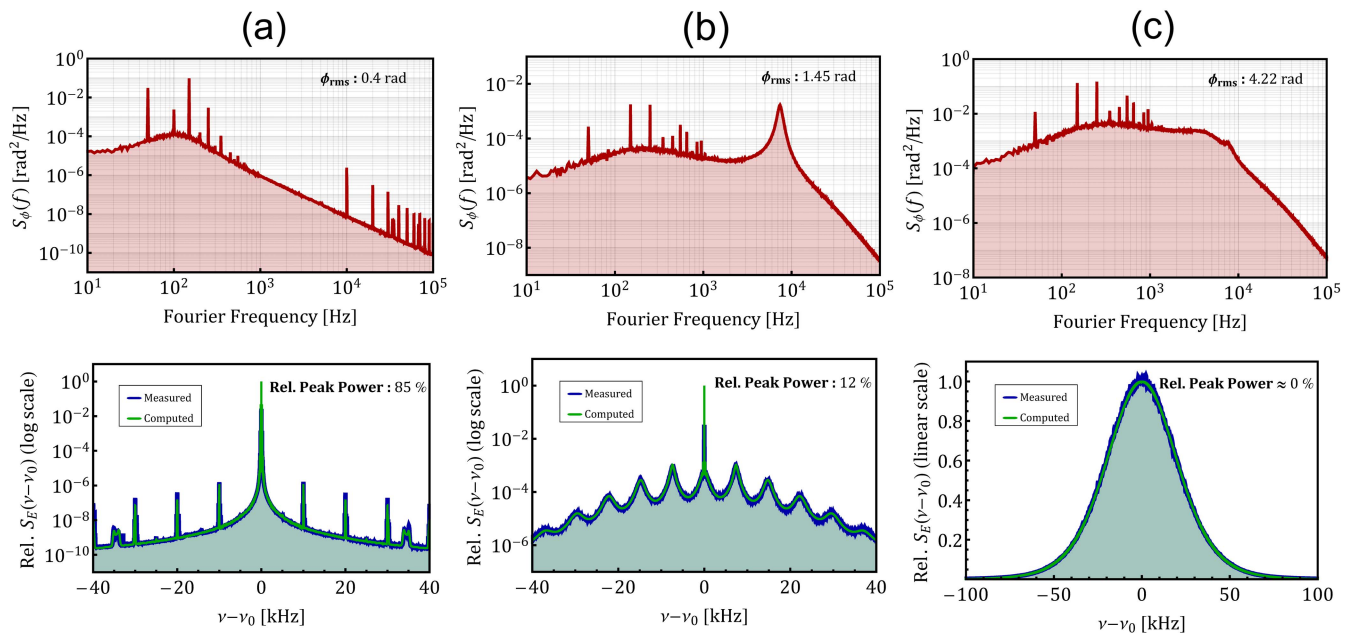


Fig. 7. Comparison of the power spectra computed using Middleton's series with experimental spectra. Top: experimental PN-PSD measured for different signals corresponding to the three regimes of (a) low, (b) intermediate, and (c) high integrated phase noise. Bottom: corresponding power spectra experimentally measured (blue traces) and computed (green traces) using Middleton's series restricted to the terms of order up to  $n_{\max}$  as given by (12). Here  $n_{\max} =$  (a) 1, (b) 7, and (c) 31.

The three reported examples represent real signals corresponding to the three characteristic regimes of phase noise where the power spectrum is made of 1) a coherent peak surrounded on both sides by the PN-PSD  $S_{\phi}(f)$  for low phase noise ( $\phi_{\text{rms}} < \pi/8$ ); 2) a sum of successive convolution products of  $S_{\phi}(f)$  around a weaker coherent peak at intermediate phase noise ( $\pi/8 < \phi_{\text{rms}} < \pi$ ); and 3) a bell-shaped (Gaussian) spectrum resulting from the multiple self-convolution products of  $S_{\phi}(f)$  at high phase noise ( $\phi_{\text{rms}} > \pi$ ). Despite the first case is well known from textbooks [22], the two other cases are easily and accurately computed using the proposed approach of Middleton's series restricted to the terms of orders up to  $n_{\max}$  given by (12). This is a significant advantage compared to the use of Elliott's general formula that is not so simple to apply in such cases.

## V. CONCLUSION

In this paper, we revisited the relationship that links the PN-PSD of a signal to its power spectrum. The exact formula has been known for a long time, and has been introduced for the first time in the field of lasers by Elliott *et al.* [16]. However, computing this formula with real phase noise data is not straightforward and can be fairly time-consuming. Indeed, it involves a double integration process, which requires a careful adjustment of two parameters, the sampling rate of the autocorrelation function and the overall range of the time delay  $\tau$ . These parameters cannot be chosen completely independently and their selection depends on the final frequency range and resolution that are targeted for the computed power spectrum, which are generally unknown *a priori*.

In this paper, we presented the high benefits offered by a different approach based on a Taylor expansion of

Elliott's formula into a series of self-convolution products of the PN-PSD that was first introduced by Middleton [10]. Despite its anteriority, Middleton's expansion series has been much less known and used than Elliott's formula to our knowledge, especially in the laser community. This is unfortunate, as the use of Middleton's expansion series offers many advantages. On a qualitative point of view, the shape of the power spectrum corresponding to an arbitrary PN-PSD can be easily understood in all different regimes of low, intermediate, and high integrated phase noise that are well known for some of them, but much less for others. Our theoretical considerations have also enabled us to better define the boundaries of these three noise regimes. On a quantitative point of view, we have theoretically and experimentally shown that only a limited number of terms of the infinite series have a significant contribution to the power spectrum. We have introduced a simple guideline given by (12) to determine these terms. This number depends only on the integrated phase noise of the signal and not on the shape of its PN-PSD. Therefore, this parameter can be easily and unambiguously determined prior to the calculation, which is not the case in the computation of Elliott's general formula. We have shown that an improper choice of the parameters used to compute Elliott's formula can lead to significant discrepancies in the computed power spectrum. Even with proper parameters, other artifacts (such as Gibbs' artifact) can result from the Fourier transform involved in Elliott's general formula. In contrast, the use of Middleton's series as proposed in this paper is very direct and does not rely on some particular choice of computational parameters.

For these reasons, we believe that the approach reported in this paper based on Middleton's series can benefit many scientists who are interested in precisely determining the

spectrum line shape of an oscillator from its PN-PSD in a simple way, instead of only getting an approximate value of its linewidth [7]. This method deserves to be considered by the laser community as a viable and simpler alternative to the computation of Elliott's general formula. In a next step, we plan to use this computational approach to quantitatively determine the domain of validity and accuracy of the linewidth approximation obtained from the  $\beta$ -separation line concept that is widely used in the laser community [7], especially in the low-noise regime where the FN-PSD approaches this limit, and to study in detail the transition from a finite linewidth to a coherent peak spectrum.

#### ACKNOWLEDGMENT

The authors would like to thank one of the anonymous reviewers of this article who provided very relevant comments during the review process, which helped to improve the quality of the paper and broadened its scope.

#### REFERENCES

- [1] S. A. Diddams *et al.*, "An optical clock based on a single trapped  $^{199}\text{Hg}^+$  ion," *Science*, vol. 293, no. 5531, pp. 825–828, Aug. 2001.
- [2] U. Sterr *et al.*, "The optical calcium frequency standards of PTB and NIST," *Comp. Rendus Phys.*, vol. 5, no. 8, pp. 845–855, Oct. 2004.
- [3] T. M. Fortier *et al.*, "Generation of ultrastable microwaves via optical frequency division," *Nature Photon.*, vol. 5, no. 7, pp. 425–429, Jun. 2011.
- [4] X. Xie *et al.*, "Photonic microwave signals with zeptosecond-level absolute timing noise," *Nature Photon.*, vol. 11, no. 1, pp. 44–47, Jan. 2017.
- [5] C. Affolderbach and G. Mileti, "A compact laser head with high-frequency stability for Rb atomic clocks and optical instrumentation," *Rev. Sci. Instrum.*, vol. 76, no. 7, p. 073108, Jul. 2005.
- [6] R. Matthey, F. Gruet, S. Schilt, and G. Mileti, "Compact rubidium-stabilized multi-frequency reference source in the 1.55- $\mu\text{m}$  region," *Opt. Lett.*, vol. 40, no. 11, pp. 2576–2579, Jun. 2015.
- [7] G. Di Domenico, S. Schilt, and P. Thomann, "Simple approach to the relation between laser frequency noise and laser line shape," *Appl. Opt.*, vol. 49, no. 25, pp. 4801–4807, 2010.
- [8] N. Bucalovic, V. Dolgovskiy, C. Schori, P. Thomann, G. Di Domenico, and S. Schilt, "Experimental validation of a simple approximation to determine the linewidth of a laser from its frequency noise spectrum," *Appl. Opt.*, vol. 51, no. 20, pp. 4582–4588, 2012.
- [9] D. Middleton, "The distribution of energy in randomly modulated waves," *London Edinburgh Dublin Philos. Mag. J. Sci.*, vol. 42, no. 330, pp. 689–707, Jul. 1951.
- [10] D. Middleton, *An Introduction to Statistical Communication Theory: An IEEE Press Classic Reissue*. Hoboken, NJ, USA: Wiley, 1996.
- [11] N. M. Blachman, "Limiting frequency-modulation spectra," *Inf. Control*, vol. 1, no. 1, pp. 26–37, 1957.
- [12] N. Abramson, "Bandwidth and spectra of phase-and-frequency-modulated waves," *IEEE Trans. Commun. Syst.*, vol. 11, no. 4, pp. 407–414, Dec. 1963.
- [13] J. L. Stewart, "The power spectrum of a carrier frequency modulated by Gaussian noise," *Proc. IRE*, vol. 42, no. 10, pp. 1539–1542, Oct. 1954.
- [14] N. M. Blachman, "A generalization of Woodward's theorem on FM spectra," *Inf. Control*, vol. 5, no. 1, pp. 55–63, 1962.
- [15] N. M. Blachman and G. McAlpine, "The spectrum of a high-index FM waveform: Woodward's theorem revisited," *IEEE Trans. Commun. Technol.*, vol. COM-17, no. 2, pp. 201–208, Apr. 1969.
- [16] D. S. Elliott, R. Roy, and S. J. Smith, "Extracavity laser band-shape and bandwidth modification," *Phys. Rev. A, Gen. Phys.*, vol. 26, no. 1, p. 12, 1982.
- [17] J. W. Cooley and J. W. Tukey, "An algorithm for the machine calculation of complex Fourier series," *Math. Comput.*, vol. 19, no. 90, pp. 297–301, 1965.
- [18] A. L. Schawlow and C. H. Townes, "Infrared and optical masers," *Phys. Rev.*, vol. 112, no. 6, p. 1940, 1958.
- [19] C. H. Henry, "Theory of the linewidth of semiconductor lasers," *IEEE J. Quantum Electron.*, vol. QE-18, no. 2, pp. 259–264, Feb. 1985.
- [20] S. W. Smith, *The Scientist and Engineer's Guide to Digital Signal Processing*. San Diego, CA, USA: California Technical Publishing, 1999.
- [21] A. Godone, S. Micalizio, and F. Levi, "RF spectrum of a carrier with a random phase modulation of arbitrary slope," *Metrologia*, vol. 45, no. 3, p. 313, 2008.
- [22] F. Riehle, *Frequency Standards: Basics and Applications*. Weinheim, Germany: Wiley, 2004.
- [23] J. W. Gibbs, "Fourier's series," *Nature*, vol. 59, no. 1522, p. 200, 1898.
- [24] J. W. Gibbs, "Fourier's series," *Nature*, vol. 59, no. 1539, p. 606, 1899.
- [25] H. Wilbraham, "On a certain periodic function," *Camb. Dublin Math. J.*, vol. 3, pp. 198–201, 1848.
- [26] M. Bôcher, "Introduction to the theory of Fourier's series," *Ann. Math.*, vol. 7, no. 3, pp. 81–152, 1906.



**Pierre Brochard** was born in Versailles, France, in 1992. He studied physics at the Université du Maine, Le Mans, France, and received the M.S. degree with highest honours in 2015. Since 2015, he has been pursuing the Ph.D. degree with the Laboratoire Temps-Fréquence, University of Neuchâtel, Neuchâtel, Switzerland, where he works on optical frequency combs and frequency-stabilized lasers.

He has authored or co-authored five articles in international peer-reviewed journals and more than 15 conference contributions.

Mr. Brochard was a member of the French Physical Society and is currently a member of the Optical Society of America.



**Thomas Südmeyer** (A'11–M'12) studied physics at Leibniz University, Hanover, Germany, and ENS, Paris, France. He received the Ph.D. degree for his research on the first mode-locked thin-disk lasers and novel nonlinear systems from Eidgenössische Technische Hochschule (ETH), Zurich, Switzerland, in 2003. He received the Habilitation degree from ETH Zurich, in 2011.

In 1999, he started his research on ultra-fast lasers during an EU fellowship at Strathclyde University, Glasgow, U.K. From 2003 to 2005, he developed industrial laser solutions at Sony Corporation, Tokyo, Japan. From 2005 to 2011, he investigated new concepts for ultrafast science and technology at ETH. In 2011, he joined the University of Neuchâtel, Neuchâtel, Switzerland, as a Full Professor and the Head of the Laboratoire Temps-Fréquence. He has authored more than 90 papers in international peer-reviewed journals, and two book chapters, and he holds or applied for ten patents. His research interests are exploring and pushing the frontiers in photonics, metrology, and ultrafast science.

Dr. Südmeyer has been the Coordinator of several Swiss and European projects and was awarded an ERC Starting Grant in 2011. He has served the research community as an Associate Editor of *Optics Express* during 2009–2015 and the IEEE PHOTONICS TECHNOLOGY LETTERS since 2014.



**Stéphane Schilt** was born in Lausanne, Switzerland, in 1970. He received the M.S. degree in physics and the Ph.D. degree in technical sciences from the Swiss Federal Institute of Technology (EPFL), Lausanne in 1994 and 2002, respectively.

From 2002 to 2005, he was a Post-Doctoral Researcher with EPFL. He was Project Manager with IR Microsystems, Lausanne, where he focused on the development of laser-based trace gas sensors. Since 2009, he has been a Senior Scientist with Laboratoire Temps-Fréquence, University of Neuchâtel, Neuchâtel, Switzerland. He has authored or co-authored two book chapters, 55 articles in international peer-reviewed journals, and more than 130 conference contributions. He holds or has applied for three patents. His research interests include optical frequency combs, optical metrology, frequency-stabilized lasers, and laser spectroscopy.

Dr. Schilt is a member of the Optical Society of America, the Swiss Physical Society, and the European Physical Society. He was a member of the Optical Metrology committee for the CLEO conference during 2015–2017, and a Committee Member for the LACSEA conference in 2016. He is currently an Associate Editor of the *Journal of Spectroscopy* and acts as a reviewer for various journals.